

Anhydrous Lithium Acetate Polymorphs and Its Hydrates: Three-Dimensional Coordination Polymers

F. J. Martínez Casado,^{*,†,‡} M. Ramos Riesco,[§] M. I. Redondo,[§] D. Choquesillo-Lazarte,[‡] S. López-Andrés,[⊥] and J. A. Rodríguez Cheda[§]

[†]BM16-Laboratori de Llum Sincrotró (LLS), c/o E.S.R.F., 6 rue Jules Horowitz, 38043 Grenoble, France

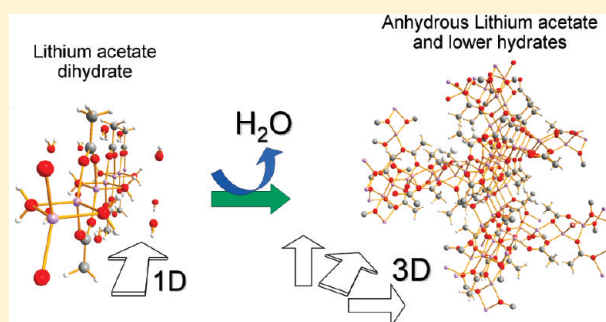
[‡]Laboratorio de Estudios Cristalográficos, IACT-CSIC, Edificio Instituto López Neyra, Avenida del Conocimiento s/n, P.T. Ciencias de la Salud, E-18100 Armilla, Granada, Spain

[§]Departamento de Química Física I, Facultad de Ciencias Químicas, Universidad Complutense, 28040 Madrid, Spain

[⊥]Departamento de Cristalografía y Mineralogía, Facultad de Ciencias Geológicas, Universidad Complutense, 28040 Madrid, Spain

 Supporting Information

ABSTRACT: Lithium acetate is a very common salt with many and varied uses. Nevertheless, only two compounds were known apparently, the anhydrous salt and lithium acetate dihydrate, but only the latter was really characterized. In this paper, two polymorphs of anhydrous lithium acetate and three novel hydrates (with lithium acetate/H₂O ratios 4:1, 7:3, and 1:1) are reported for the first time, besides the well-known lithium acetate dihydrate. The five new compounds are three-dimensional (3D) coordination polymers, different from the one-dimensional (1D) structure of lithium acetate dihydrate. The structures and the relative stability of the two anhydrous lithium acetate polymorphs are also compared. The compounds were studied by single crystal X-ray diffraction (SCXRD), powder X-ray diffraction (PXRD), differential scanning calorimetry (DSC), thermogravimetric analysis (TGA), and infrared spectroscopy (FTIR).



1. INTRODUCTION

Studies in the area of coordination polymers or metal–organic frameworks (MOFs) have been carried out for a long time, and their designable architectures for potential application as functional materials have led to an explosion in research in the past decade.^{1–5} It has been reported that MOFs can be applied in gas storage, gas separation, ion exchange, and selective adsorption of organic and inorganic molecules.^{6–10}

Lithium acetate (hereafter referred to as LiC₂) is a very common salt of great importance due to its many and varied uses, such as (a) product for drug formulation and therapy,^{11–13} (b) buffer for gel electrophoresis of DNA and RNA,¹⁴ (c) additive or catalyst for textiles and polymer production,^{15,16} (d) precursor material for batteries^{17–23} and ferromagnetic nanoparticles,²⁴ (e) product for efficient yeast transformation,^{25–27} lithium-6 CP/MAS standard,²⁸ solvent,²⁹ catalyst,³⁰ etc. In this study, we describe LiC₂ and some of its hydrates forming different three-dimensional (3D) microporous frameworks.

There are currently two known forms of LiC₂: anhydrous and dihydrate, both commercially available. Only Saunderson et al., by single crystal X-ray diffraction (XRD), have reported the structure of an anhydrous form,³¹ only giving information about its unit cell, and ruling out the possibility of the existence of a lower hydrate than the well-known dihydrate. Additionally,

anhydrous LiC₂, together with other dried members of the lithium alkanoate series, have been systematically and thoroughly studied by adiabatic calorimetry and differential scanning calorimetry (DSC) by Ferloni, Franzosini and Westrum.^{32–34} These studies showed a rather simple stepwise melting process from the totally ordered crystal, at very low temperatures, up to the isotropic liquid, in comparison with other metal alkanoate series (e.g., thallium(I) or lead(II) alkanoates).^{35–37}

On the other hand, lithium acetate dihydrate has been fully characterized. The structure was determined by single crystal XRD and powder neutron diffraction, showing the formation of a one-dimensional (1D) coordination polymer.^{38–41} This hydrate was also analyzed by calorimetric and spectroscopic measurements,^{42–44} and it was also used to study the methyl group as a quantum rotor. Its structure has been very suitable for testing the standard theory of methyl group rotation,^{41,45–48} studying the translational/rotational coupling of the hindered CH₃ quantum-rotor,⁴⁷ and the transitions attributed to quantum-rotational tunneling⁴⁸ by inelastic neutron scattering.

Received: August 2, 2010

Revised: February 5, 2011

Published: March 07, 2011

Table 1. LiC₂/H₂O Ratio and Empirical Formula of the Different Compounds Studied

compound	anh. LiC ₂ - 1A	anh. LiC ₂ - 1B	2	3	4	5
LiC ₂ /H ₂ O ratio	1:0	1:0	4:1 (1:0.25)	7:3 (1:0.429)	1:1	1:2
empirical formula	15(LiC ₂ H ₃ O ₂)	108(LiC ₂ H ₃ O ₂)	4(LiC ₂ H ₃ O ₂) · H ₂ O	7(LiC ₂ H ₃ O ₂) · 3H ₂ O	4(LiC ₂ H ₃ O ₂) · 4H ₂ O	LiC ₂ H ₃ O ₂ · 2H ₂ O

Table 2. Methods for Obtaining the Different LiC₂ Hydrates by Slow Evaporation in Different Solvents and Mixtures, or by Hydration at Ambient Conditions

method	compounds formed
isopropanol–methanol (1:1)	2, 5
isopropanol–methanol (7:3)	2, 3, 5
isopropanol–methanol (9:1)	5
methanol	5
isopropanol	5
ethanol–isopropanol (1:1)	3, 5
ethanol–ether (1:1)	3, 5
from 1A (hydration in ambient conditions)	2, 3, 4
from 1B (hydration in ambient conditions)	5

Lithium formate presents two hygroscopic anhydrous polymorphs^{49,50} and seems to be the only homologous compound that exists as a hydrate (monohydrate, which is a piezoelectric material).^{51,52} Members of the lithium alkanoates series with an alkyl chain of three or more carbon atoms are anhydrous and non-hygroscopic, as has been recently reported on the structure of lithium propionate, butanoate, and pentanoate.^{53–55} These compounds present a bilayered (ionic and lipidic) arrangement, typical of metal alkanoates, and also similar for lithium halogenoacetates.⁵⁶

In this work, six different compounds, two polymorphs of anhydrous LiC₂ and four lithium acetate hydrates, are studied, being five of them reported for the first time. Their LiC₂/H₂O ratio, formula, and name used through out this article are summarized in Table 1.

2. EXPERIMENTAL SECTION

2.1. Sample Preparation. *Anhydrous LiC₂ Polymorphs.* Crystals of anhydrous LiC₂ polymorph **1A** were obtained by heating commercial LiC₂, or any of the hydrates, in a hot stage above the dehydration temperature and up to the melting point of the anhydrous salt, and then cooling the melt very slowly (0.1 K·min^{−1}) to 473 K. Tiny single crystals of the other polymorph of anhydrous LiC₂ (**1B**) were obtained by drying crystals of compound **5** at 428 K for 2 h. For both polymorphs, the crystals were covered with Paratone to avoid hydration.

LiC₂ Hydrates. The different LiC₂ hydrates can be obtained by hydration of both anhydrous LiC₂ forms, which are highly hygroscopic, or by slow evaporation from solutions of compound **5** (lithium acetate dihydrate), using different solvents, or mixtures of them. Crystals suitable for X-ray studies were grown up by slow evaporation from these solutions. However, the ratio of each compound depends on the evaporation rate from each solution, which favors obtaining of compound **5** at fast evaporation rates in all of the cases. The methods for obtaining the hydrates, compounds **2–5**, are shown in Table 2.

Anhydrous lithium acetate and lithium acetate dihydrate were purchased from Aldrich, 99.95% and 99.999% purity, respectively. The solvents used in this work were isopropanol (Merck, ≥99.7%), methanol (Merck, ≥99.8%), ethanol (Merck, ≥99.8%), and ether (Fluka, >99.8%).

2.2. Single Crystal X-ray Diffraction (SCXRD). Measurements were conducted using synchrotron radiation (with $\lambda = 0.7379$, 0.9803, and 0.7514 Å for compounds **1A**, **1B**, and **2**, respectively, and 0.7293 Å, for the others) at the BM16 Spanish beamline of ESRF with a CCD detector (ADSCQ210rCCD), making phi scans when collecting the data. The oscillation range ($\Delta \phi$) used for each image was one degree, for compounds **1** (**1A** and **1B**) to **4**, and two, for compound **5**. Compounds **1A** and **2** were measured at 100 and 298 K, and the others at 100 K.

The structures were solved by direct methods and subsequent Fourier syntheses using the SHELXS-97 program,⁵⁷ and were refined by the full-matrix least-squares technique against F^2 , using the SHELXL-97 program, and XLMP (multi processor version of SHELX), in the case of compound **1B**, with many parameters to be refined.⁵⁷ Anisotropic thermal parameters were used to refine all non-H atoms. Hydrogen atoms of water molecules were located in the Fourier difference map. The other H atoms were placed in idealized positions, and their parameters were not refined.

The experimental parameters, crystal sizes, and main crystallographic data for the compounds studied are shown in Table 3.

Further crystallographic details for the structures reported in this paper may be obtained from the Cambridge Crystallographic Data Center (see Supporting Information).

2.3. Powder X-ray Diffraction (PXRD). Laboratory X-ray powder diffraction patterns were collected on a PANanalytical X'Pert Pro MPD diffractometer equipped with vertical goniometer theta/theta (Cu K α 1 radiation, 1.54056 Å, Ni filter, PIXcel detector and with a programmable divergence slit for line focus and a programmable antiscatter slit).

Thermodiffraction experiments were carried out with a Philips X'Pert PRO MPD X-ray diffractometer with vertical goniometer θ/θ (Cu K α 1 radiation, 1.54056 Å, Ni filter, X'Celerator detector, equipped with a high-temperature chamber Anton Paar HTK1200. In-situ XRD area was scanned from $2\theta = 2–50^\circ$ at several temperatures in the range from 273 to 500 K during the heating and the cooling, at a rate of 3 K·min^{−1}.

2.4. Differential Scanning Calorimetry (DSC). A TA Instruments DSC, model Q10, connected to a RCS cooling unit, was used to register all the thermograms. Tightly sealed aluminum volatile pans were used, in dry nitrogen, flowing at 50.0 mL·min^{−1}. A MTS Mettler microbalance was used to weigh the samples, ranging between 3 and 10 mg (with an error of ± 0.001 mg). The calorimeter was calibrated in temperature using standard samples of In and Sn, supplied by TA (purity >99.999% and >99.9%, respectively), and of benzoic acid (purity >99.97%), supplied by the former NBS (lot 39i), and in enthalpy with the In and Sn standards already described.

2.5. Thermogravimetric Analysis (TGA). TGA was carried out on a Delta Series TA-SDTQ600 in nitrogen atmosphere (flowing at 100.0 mL·min^{−1}) from room temperature to 600 K (at a heating rate of 5 K·min^{−1}) using platinum crucibles.

2.6. Infrared Spectroscopy (FTIR). FTIR measurements were carried out with a Perkin-Elmer Spectrum 100 spectrometer, at room temperature, using a Universal ATR diamond/ZnSe accessory.

3. RESULTS

3.1. Structural Analysis. Six compounds were studied in this work based on lithium acetate (LiC₂): two polymorphs of anhydrous LiC₂ and four different hydrates. The composition

Table 3. Experimental Parameters and Main Crystallographic Data for the Studied Compounds

data	anh. LiC ₂ poly. 1		anh. LiC ₂ poly. 2	4LiC ₂ ·H ₂ O		7LiC ₂ ·3H ₂ O	4LiC ₂ ·4H ₂ O	LiC ₂ ·2H ₂ O
compound	1A		1B	2		3	4	5
empirical formula	Li ₁₅ C ₃₀ H ₄₅ O ₃₀		Li ₁₀₈ C ₂₁₆ H ₃₂₄ O ₂₁₆	Li ₄ C ₈ H ₁₄ O ₉		Li ₇ C ₁₄ H ₂₆ O ₁₇	Li ₄ C ₈ H ₂₀ O ₁₂	LiC ₂ H ₇ O ₄
<i>M_r</i> (g·mol ^{−1})	989.76		7126.27	281.95		514.93	336.00	102.01
crystal system	monoclinic		triclinic	triclinic		triclinic	monoclinic	orthorhombic
space group (No.)	<i>P</i> 2 ₁ / <i>n</i> (14)		<i>P</i> $\bar{1}$ (2)	<i>P</i> $\bar{1}$ (2)		<i>P</i> $\bar{1}$ (2)	<i>P</i> 2 ₁ / <i>c</i> (14)	<i>Cmmm</i> (65)
crystal size (mm)	0.05 × 0.035 × 0.020		0.040 × 0.030 × 0.020	0.10 × 0.08 × 0.05		0.07 × 0.05 × 0.03	0.04 × 0.03 × 0.02	0.10 × 0.08 × 0.02
temperature (K)	100(2) 298(2)		100(2)	100(2) 298(2)		100(2)	100(2)	100(2)
<i>a</i> (Å)	20.027(4) 20.424(4)		23.488(5)	6.7360(13) 6.8070(14)		7.6890(15)	7.0870(14)	6.7340(13)
<i>b</i> (Å)	12.024(2) 12.081(2)		27.709(6)	9.5030(19) 9.5690(19)		11.959(10)	14.514(3)	10.885(2)
<i>c</i> (Å)	22.675(5) 22.735(5)		29.963(6)	12.284(3) 12.284(3)		13.881(17)	15.298(3)	6.5650(13)
α (°)	90 90		99.59(3)	69.85(3) 69.77(3)		72.28(3)	90	90
β (°)	107.23(3) 107.92(3)		91.80(3)	78.43(3) 78.89(3)		88.93(3)	99.80(3)	90
γ (°)	90 90		106.93(3)	72.80(3) 78.89(3)		89.08(3)	90	90
<i>V</i> (Å ³)	5215.3(18) 5337.7(18)		18329(6)	700.9(2) 713.4(3)		1215.5(4)	1550.6(5)	481.21(16)
<i>Z</i>	4 4		2	2 2		2	4	4
λ (Å)	0.7379 0.7379		0.9803	0.7514 0.7514		0.7293	0.7293	0.7293
<i>D_c</i> (g·cm ^{−3})	1.261 1.232		1.291	1.336 1.313		1.407	1.439	1.408
μ (mm ^{−1})	0.11 0.10		0.11	0.12 0.11		0.12	0.13	0.08
reflection collected	13566 12588		32209	4139 3401		6984	3758	333
reflections with <i>I</i> > 2σ(<i>I</i>)	12762 11031		25960	3991 3366		6742	3433	328
parameters refined	677 677		4861	199 209		448	298	34
hydrogen treatment	not refined not refined		not refined	mixed mixed		mixed	mixed	mixed
<i>R</i> -factor	0.0354 0.0504		0.0749	0.048 0.050		0.038	0.045	0.035
<i>wR</i> -factor	0.0961 0.1415		0.2071	0.137 0.127		0.109	0.128	0.079
goodness of fit	1.023 1.051		1.010	0.929 1.053		0.918	0.996	1.112
CCDC deposition nos.	770300 770301		802905	739978 739979		739980	739976	739977

of each compound is given in Table 1. Structures for compounds **1** (A and B) to **5** were solved by SCXRD, **1**–**4** being reported for the first time.

Structures of compounds **1A** and **4** are monoclinic, and compounds **1B**, **2**, and **3** are triclinic. The main characteristic of all of these compounds is the fact that they are 3D coordination polymers. Special attention must be paid to the huge unit cell of **1B**, with 108 independent LiC₂ molecules (and *Z* = 2), with a pseudohexagonal packing. Compound **5** was solved as orthorhombic (*Cmmm*), as already known, showing 1D arrays linked with H bonds from zeolitic water molecules. In every case, each Li ion is coordinated by four oxygens, forming a regular tetrahedral. The structure of compounds **1** (A and B) to **5** and a 3D representation of the crystal architecture (with the tetrahedral coordination of Li atoms in blue polyhedra) of all these salts are shown in Figures 1–6.

The ionic structures in all of the compounds consist of rings formed by Li and O atoms (4-membered rings) or Li, O, and C atoms (5-, 6-, and 8-membered rings). The appearance of these rings decreases as the water content increases. Thus, the resemblance is clear between both anhydrous LiC₂ and lower hydrates, especially with compound **2** (Table 4). In this sense, compound **1A** can be obtained by dehydration of compound **2**, as detected by powder XRD. On the other hand, compound **5**, shows a perpendicular arrangement of 4 and 8 membered planar rings, forming the 1D structure, in contrast to the other compounds, with rings out of the plane forming the 3D structures.

The water present in the hydrates **2**–**4** is coordination water, while in the case of compound **5** there are both coordination and

hydration (zeolitic) water molecules. Water molecules in the different hydrates can be compared by means of their coordination (lone pairs of the O atom) and hydrogen bonds (Table 4).⁵⁸ Only in the case of compound **5**, the water molecules with both lone pairs of the oxygen atom coordinate two Li atoms in a tetrahedral configuration, whereas only one Li atom is coordinated in the other hydrates (trigonal and pyramidal coordination). Regarding the hydrogen bonds, these are mostly linear (O–H···O) and asymmetric, but only in the case of compound **5** are symmetric (see ref 58).

The most relevant aspects of the structure of each compound are briefly given below.

Compound 1A. Its cell is monoclinic, *P*₂₁/*n*, with 15 independent Li and acetate (C₂) ions in the asymmetric unit. A variety of Li–O and Li–O–C rings (in the plane, *p*, and out of the plane, *op*) is found in the structure. Li–O quadrilaterals appear isolated and also in blocks of three of them (joined by the vertices, sharing the lithium atoms). Other membered Li–O–C rings (*S_p*, *S_{op}*, *6_{op}*, and *8_{op}*) complete the 3D framework. In addition, very small channels are formed between the (2 0 $\bar{2}$) and (2 0 0) planes. Li centers are linked by μ_3 - and μ_4 -acetate ligands. The simplified structure can be interpreted as a stacking of planes (2 0 $\bar{2}$), full 2D ionic networks presenting the most intense diffraction peak, joined between them by units of one quadrilateral (with two Li7 atoms) and a block of three (with two of each Li15 and Li14 atoms).

Compound 1B. This polymorph presents a large triclinic unit cell (*P* $\bar{1}$), and the asymmetric unit presents 108 independent Li and C₂ ions and is constituted by 27 different blocks of three

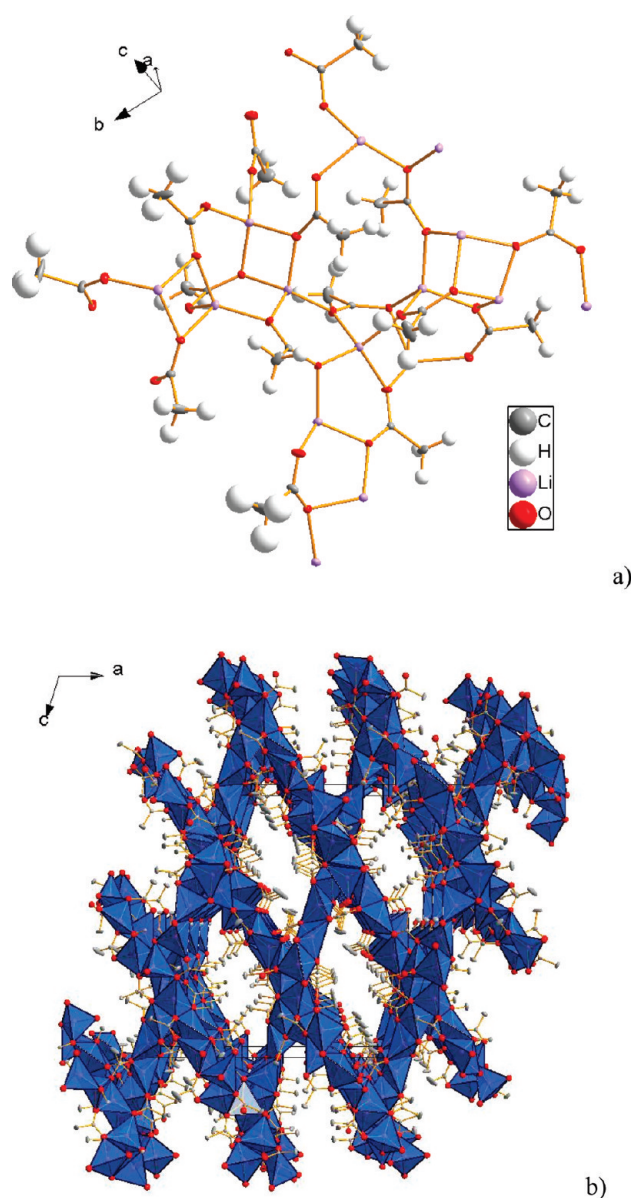


Figure 1. (a) Fragment of polymeric compound 1A (stable polymorph of anhydrous LiC_2 , at 100 K) showing 50% probability displacement ellipsoids; (b) projection in the ac plane, showing the 3D architecture (H atoms omitted for clarity).

Li-O quadrilaterals joined by the vertices (see Figure 2a). Every Li atom in this structure belongs to one of these blocks, each of them presenting 4 Li atoms, practically aligned. These blocks are intertwined and build the pseudo-hexagonal 3D network (view along the a axis), forming micropores, between the $(0\ 3\ 0)$, $(0\ 1\ 3)$ and $(0\ \bar{2}\ 3)$ planes. Differently from 1A, here there are no isolated quadrilaterals. As in the former polymorph, the crossing blocks also form diverse membered Li-O-C rings (S_p , S_{op} , 6_{op} , and 8_{op}). As in 1A, Li atoms are joined by μ_3 - and μ_4 -acetates. It is also noteworthy that the three mentioned atoms planes present the biggest diffraction intensities in this compound and have a similar d -spacing value as the $(2\ 0\ \bar{2})$ plane in compound 1A.

Compound 2. The unit cell is triclinic ($P\bar{1}$), and four independent Li and C_2 ions and one water molecule is found in it ($Z=2$). Aqua and μ_3 - and μ_4 -acetate ligands are found in this coordination polymer. As in the case of 1A, this compound

presents an isolated Li-O quadrilateral and a block of three, as well as other Li-O-C rings (S_{op} , 6_{op} , and 8_p). The Li atoms in the isolated quadrilaterals (Li3) are the ones coordinated by the water molecules. The second most intense Bragg peak in this compound, $(0\ 1\ 0)$, also presents a similar d -spacing value as the indicated for 1A and 1B.

Compound 3. This compound is also triclinic ($P\bar{1}$), with seven Li and C_2 ions and three water molecules in the asymmetric unit. Only isolated quadrilaterals are present in this structure, besides S_{op} and 8_{op} Li-O-C rings. There is only one O atom (O14) not coordinating any Li (this feature only appears in this compound), and three water molecules form H-bonds with it (2 of O1w and one O3w). The other water molecule (O2w) coordinates Li2 and form H-bonds with O3w and O3 . Thus, aqua, acetate (in monodentate bridging mode), and μ_3 - and μ_4 -acetate ligands appear in this compound.

Compound 4. This hydrate shows a monoclinic cell ($P2_1/c$), and four Li and C_2 ions and four water molecules form the asymmetric unit. Only S_p and S_{op} Li-O-C rings appear in this compound. Six water molecules (O1w , O2w , and O3w , twice each) are grouped and show H-bonds between them and other O atoms, while other one (O4w) coordinates Li3 atom and forms H-bonds with oxygen atoms (O4 and O6) from other acetate anions. The ligands coordinating Li atoms are aqua, and μ_2 - (in *syn-anti* mode), μ_3 - and μ_4 -acetates.

Compound 5. LiC_2 dihydrate is the most different hydrate of all the studied in this work. The unit cell is orthorhombic ($Cmmm$), and only one Li and C_2 ions and two water molecules form the asymmetric unit. Only Li-O quadrilaterals and octagons, both in the plane and joined consecutively, appear and form this 1D coordination polymer. This is the only hydrate presenting hydration water molecules, which join (by H-bonds) the 1D arrays formed by the Li atoms, acetates, and the coordination water molecules. The acetates between different arrays present a particular antiparallel packing. Li atoms are uniquely linked by μ_2 -aqua and μ_2 -acetate (in *syn-syn* mode) ligands. This compound exhibits the simplest crystal arrangement, in contrast to the anhydrous polymorphs or hydrates of LiC_2 , which present a more intricate architecture.

3.2. Thermal Analysis (DSC and TGA). A thorough thermal analysis was carried out to study the temperatures and enthalpies of transitions. The first process occurring on heating for compounds 2–5 is the dehydration, which starts at different temperatures depending on the type of water molecules in the compounds (hydration or coordination water). Thus, the water loss starts at around 330 K for compound 5 (hydration water molecules), ending around 440 K (coordination water). In the other cases, for compounds containing only coordination water molecules, the water loss occurs at around 400 K. These processes were studied by TGA, as shown in Figure 7.

After the water loss, only the melting process is detected on heating, but two different fusion peaks were observed depending on the thermal treatment, confirming the presence of polymorphism for anhydrous LiC_2 , which will be discussed later. Another important characteristic of LiC_2 is its ability to form glasses. In this sense, vitreous lithium acetate can be obtained by cooling the melt fast, and also by vacuum dehydration of LiC_2 dihydrate, even at a rather low temperature (330 K), yielding amorphous lithium acetate. This latter rather unusual method has been also reported for magnesium acetate.⁵⁹

Some of the DSC measurements carried out in these samples are shown in Figure 8 (discussed later) showing the two fusions,

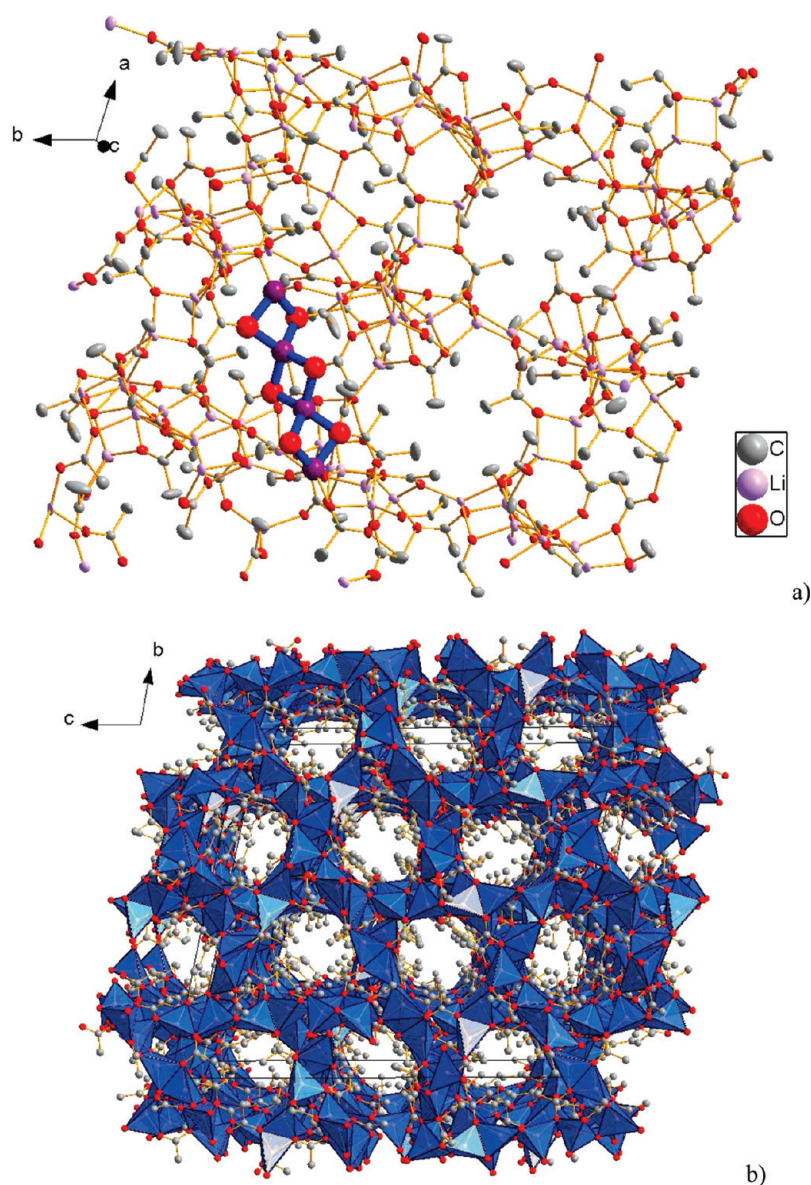


Figure 2. (a) Fragment of polymeric compound **1B** (metastable polymorph of anhydrous LiC_2), showing 50% probability displacement ellipsoids; one block of three Li–O quadrilaterals joined by the vertices is highlighted; (b) projection in the bc plane, showing the 3D crystal structure (H atoms omitted for clarity in both figures).

Table 4. Coordination of Water Molecules and Types of Hydrogen Bonds in the LiC_2 Hydrates

compound	Li–O or Li–O–C rings ^a	coordination of water	hydrogen bonds ^b
1A	$4_p, 4_{op}, 5_p, 5_{op}, 6_{op}, 8_{op}$		
1B	$4_p, 4_{op}, 5_p, 5_{op}, 6_{op}, 8_{op}$		
2	$4_p, 4_{op}, 5_{op}, 6_{op}, 8_p$	trigonal	linear, asymmetric
3	$4_p, 4_{op}, 5_{op}, 8_{op}$	pyramidal	linear, asymmetric
4	$5_p, 5_{op}$	pyramidal and trigonal	linear, asymmetric
5	$4_p, 8_p$	tetrahedral	linear, symmetric

^a p: in the plane; op: out of the plane. ^b L: linear, asym: asymmetric, sym: symmetric.

the glass transition and the crystallization processes. The thermal data for these transitions are given in Table 5.

3.3. FTIR Spectroscopy. In order to confirm the presence of water and its kind of bonding, FTIR measurements were conducted for compounds **1B**, **2**, and **5**, at room temperature

(Figure 9). In this case, compound **1B** was obtained after drying compound **5** at 423 K during 16 h. Two bands at 3455 and 3328 cm^{-1} (OH stretching) are observed for compounds **2** and **5**, indicating the presence of coordinating water molecules. In the case of compound **2**, also a band at 1651 cm^{-1} (HOH

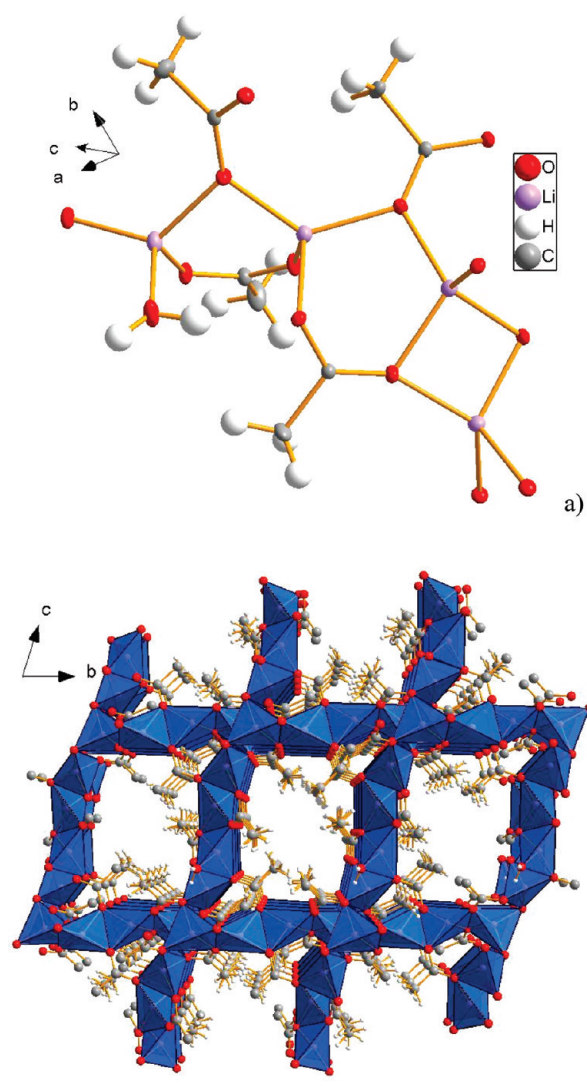


Figure 3. (a) Fragment of polymeric compound 2 ($4\text{LiC}_2/\text{H}_2\text{O}$, at 100 K) showing 50% probability displacement ellipsoids; (b) projection in the bc plane, showing the 3D architecture.

deformation) is detected. A broad band centered at 3138 cm^{-1} is observed for compound 5 due to the presence of hydration water molecules, confirming the existence of two kinds of water molecules in the room temperature commercial hydrate (compound 5). Obviously, all of these bands disappear for compound 1B.

4. DISCUSSION

Comparison of the Compounds. Most of the samples obtained from the different crystallizations, carried out in order to obtain single crystals of the different compounds, showed a mixture of all of them (hydrated samples, 2–5), varying the ratio of all of them, depending on the evaporation rates, as it has been indicated before. In this sense, compound 4 could not be isolated from this mixture. The complex structural relationship between the salts, revealed by their similarities or differences in the atomic arrangement, becomes evident even in the methods for obtaining them. Thus, for example, hydration of compound 1A in ambient conditions (293 K and relative humidity of 40%) yields the

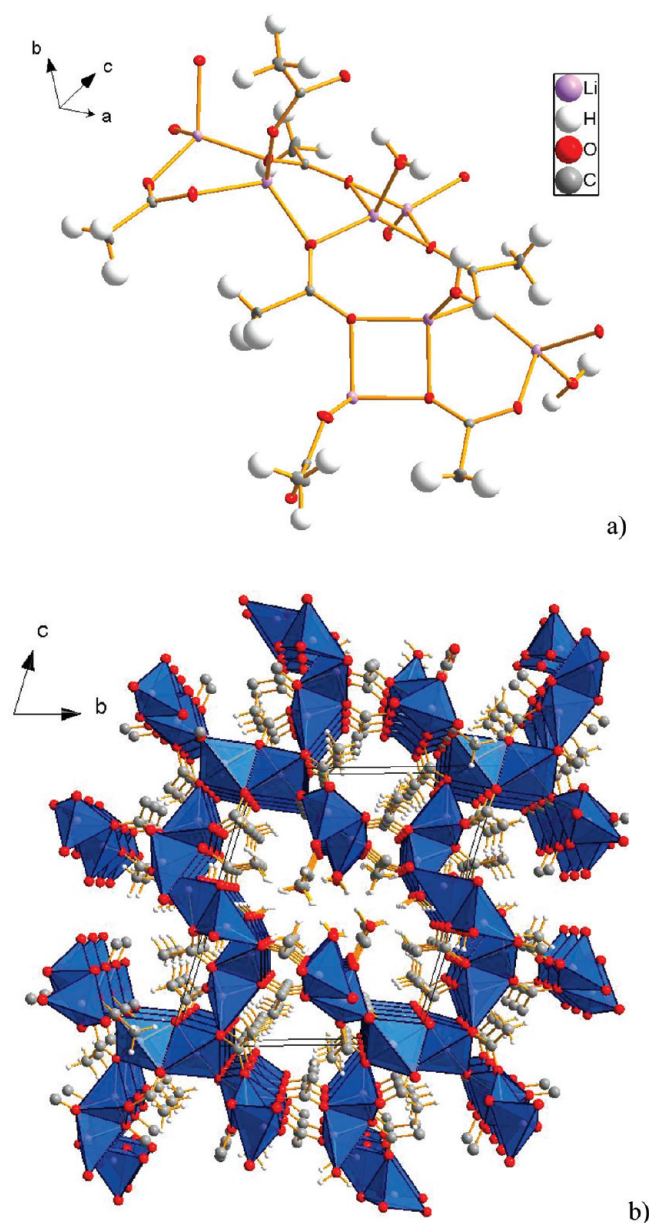


Figure 4. (a) Fragment of polymeric compound 3 ($7\text{LiC}_2/3\text{H}_2\text{O}$) showing 50% probability displacement ellipsoids; (b) projection in the bc plane, showing the 3D MOF.

formation of hydrates 2, 3, and 4, and probably other hydrates (in one week approximately), while compound 1B converts into compound 5 in the same conditions in 16 h (see Table 2). In addition, polymorphs 1A and 1B are formed respectively by dehydration of compounds 2 and 5. Consequently, although a direct relationship between compounds 1A and 2, and between 1B and 5, could be established, the comparison between the structures does not suggest this at all, mostly, between 1B and 5.

As it is explained in Section 3.1, the ionic structures consist of different sized Li–O or Li–O–C rings. This analysis suggests a clear resemblance between anhydrous LiC_2 polymorphs and lower hydrates, and, thus, all of the compounds present a 3D coordination structure, except compound 5, which forms 1D arrays.

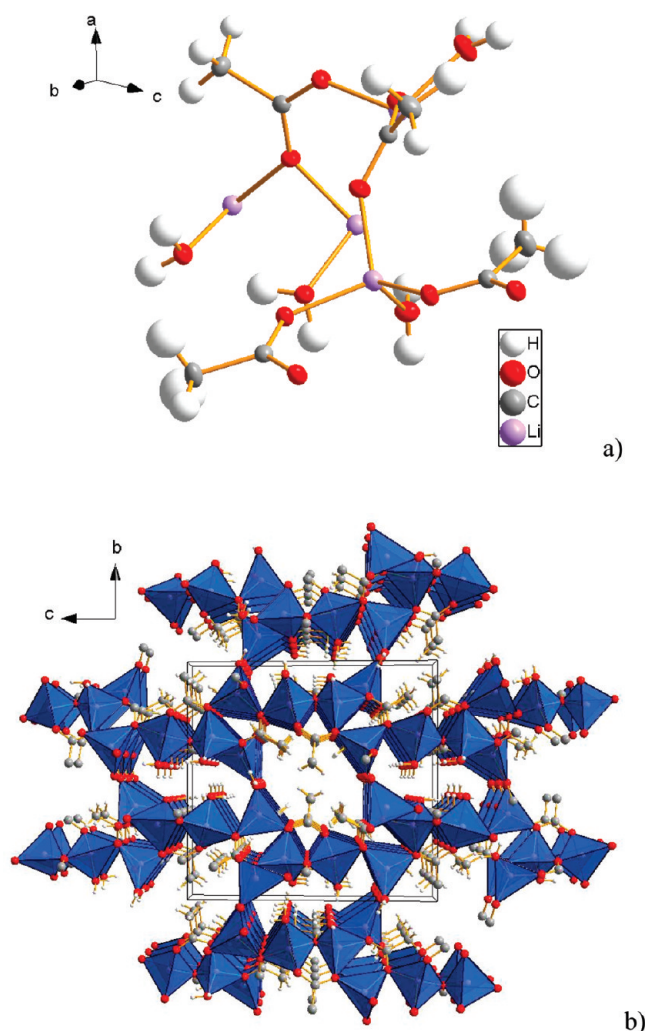


Figure 5. (a) Fragment of polymeric compound 4 ($4\text{LiC}_2/4\text{H}_2\text{O}$) showing 50% probability displacement ellipsoids; (b) projection in the bc plane, showing the 3D network.

The simulated radial distribution functions (RDFs) were used for comparison of compounds **1** (A and B) to **5**, through the packing and density of isotropic interatomic distances. These RDFs between all atoms and for selected atomic pairs were calculated from the cif files using the PDFgui program.⁶⁰ RDFs at short distances are shown in Figure 10a for the six compounds, between all atoms and between two selected atom pairs, Li–O and C–C. Significant differences are observed between compound **5** and the others, as can be inferred from the distances marked in the simulations, such as the sharp O–H bond (in the water molecules), or the $\text{O}_{\text{w1}}-\text{O}_{\text{w2}}$ distance between the coordinating and the zeolitic water molecules. Representative differences between compound **5** and the other forms lie in the antiparallel packing of the acetate anions (C–C distance in Figure 10a) and in a larger Li–O–C angle (141° , giving a longer Li–O distance, in Figure 10a). The RDFs plot also shows similarities in the density of distances between anhydrous LiC_2 **1A** and compound **2**, as expected from the ionic arrangement and related to the rapid formation of the latter by hydration of the former.

Distances in both polymorphs, **1A** and **1B**, are compared in Figure 10b, where practically the same peaks are found from the radial distribution functions between all atoms and between the

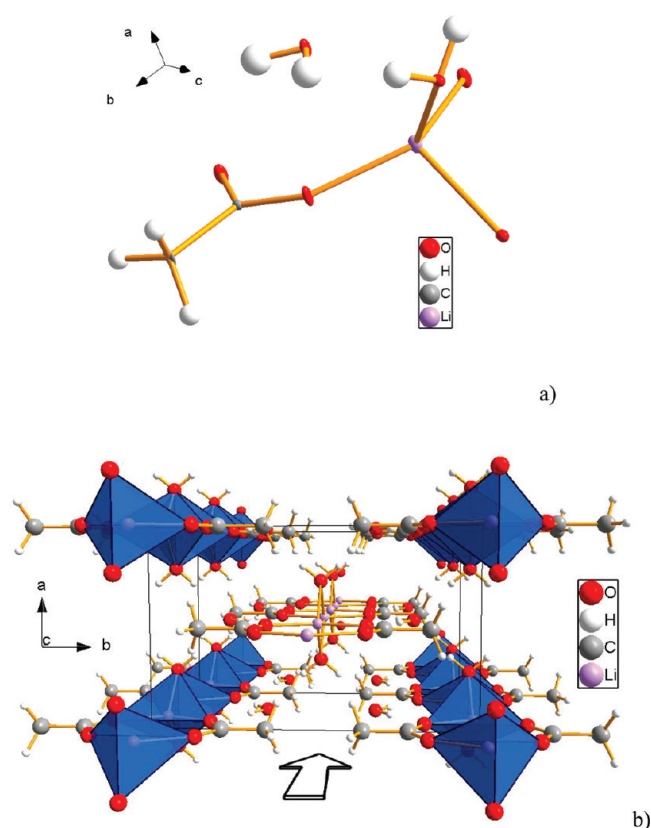


Figure 6. (a) Fragment of polymeric compound 5 ($\text{LiC}_2/2\text{H}_2\text{O}$) showing 50% probability displacement ellipsoids; (b) projection in the ab plane, showing the 1D arrays along the c axis.

indicated ones. Despite the differences in unit cell volumes between them, a similar arrangement in the Li–O and Li–O–C rings is found, and micropores are formed in both cases, as it has been indicated before, separating the ions and the lipidic tails. It is important to note that the structure changes dramatically from these compounds to other lithium alkanoates with one or more carbon atoms in the alkyl chain.^{53–55} Thus, they change from 3D to 2D MOFs, that is, the typical bilayerd structure of metal alkanoates.

Monotropic Polymorphism in Anhydrous LiC_2 . Besides the new hydrates found, the existence of two polymorphs of the anhydrous salt, as in the case of lithium formate,^{49,50} is one of the main features of LiC_2 , as proved by DSC and X-ray diffraction. The polymorphism is monotropic since the endothermic transition of one polymorph into the other is not observed by DSC on heating, as it happens with copper(II) decanoate.⁶¹

Two melting points were measured by DSC, at 560.1 and 555.7 K (with enthalpies of 13.09 and 12.89 $\text{kJ}\cdot\text{mol}^{-1}$, respectively) corresponding to the fusion of each polymorph of anhydrous LiC_2 (**1A** and **1B**). The polymorph with lower melting point and enthalpy, considered the metastable form in all the temperature range,⁶² corresponds to compound **1B**. DSC experiments were carried out to explain the formation of both polymorphs (Figure 8). Compound **2** (LiC_2 quarter-hydrate) mainly forms the stable polymorph (**1A**) after a dehydration process, at 10 $\text{K}\cdot\text{min}^{-1}$ (Figure 8a), while compound **5** (LiC_2 dihydrate), once dehydrated at 428 K for 2 h and cooled down, leads to the formation of **1B** (Figure 8c). In this sense, commercial anhydrous lithium acetate, probably obtained by dehydration

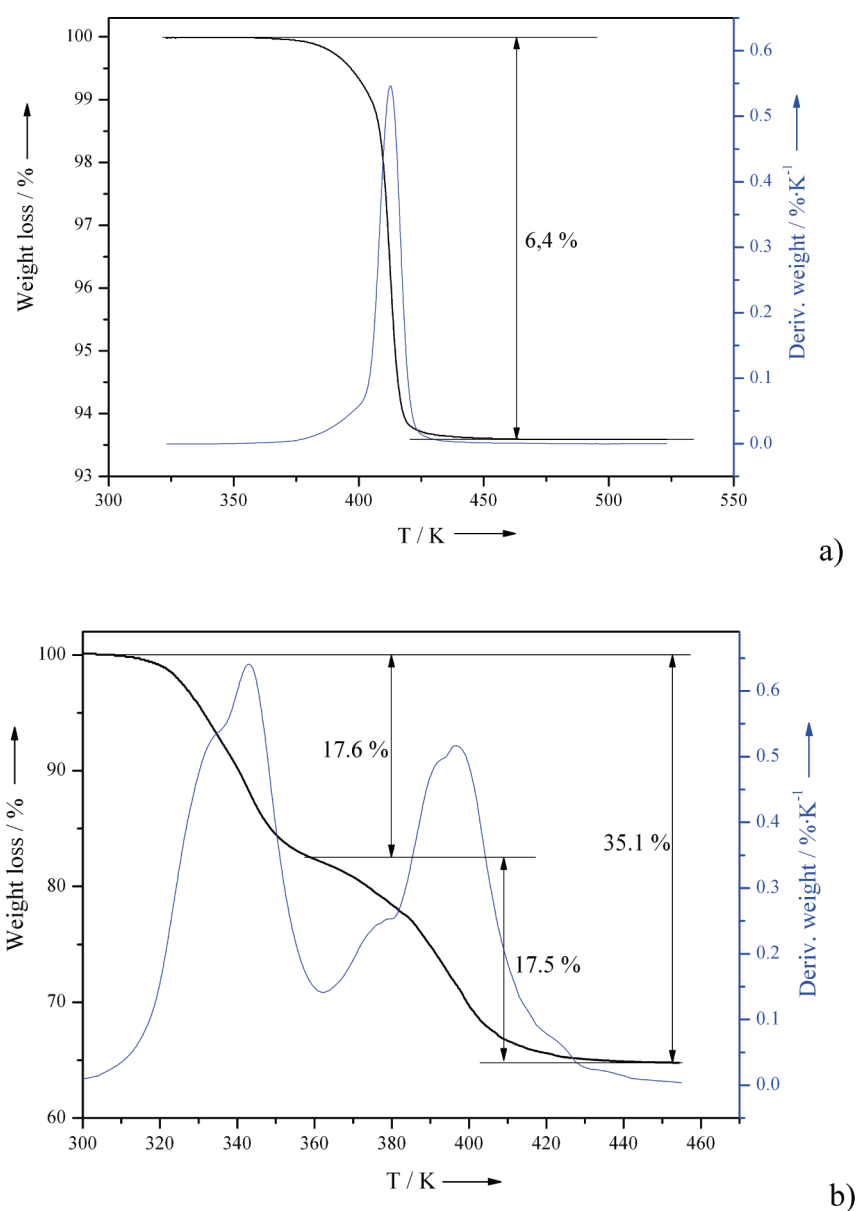


Figure 7. Weight loss (water) of compounds (a) **2** and (b) **5**, at a heating rate of $5 \text{ K} \cdot \text{min}^{-1}$.

of commercial LiC_2 dihydrate, presents the lower melting point, T_f (**1B**), and the X-ray diffractogram of **1B**, being able to assign it clearly to polymorph **1B**, that is, the metastable polymorph. On the other hand, the method for obtaining crystals of polymorph **1A** leads to a sample with the highest melting point and enthalpy (Figure 8d), the stable polymorph.

A vitreous state of anhydrous LiC_2 can be also obtained by cooling the melt (at a cooling rate of $10 \text{ K} \cdot \text{min}^{-1}$ or higher). A glass transition is found (T_g) and two crystallization processes: *crys1* and *crys2*. Thus, *crys1* would correspond to the formation of **1B**, from the undercooled isotropic liquid after the glass transition, and *crys2*, with a very small energy ($0.33 \text{ kJ} \cdot \text{mol}^{-1}$ at $10 \text{ K} \cdot \text{min}^{-1}$), to the conversion of **1B** into **1A** (Figure 8b).

Besides these calorimetric data, slurry crystallization experiments^{63,64} were carried out in order to check the stability of each polymorph. A metastable polymorph may often be obtained first during crystallization process, according to Ostwald's rule.⁶⁵ An efficient method to discover the most stable polymorph is the

Table 5. Temperatures, Enthalpies, and Entropies of the Transitions^a

process	T/K	$\Delta H/\text{kJ} \cdot \text{mol}^{-1}$	$\Delta S/\text{kJ} \cdot \text{mol}^{-1} \cdot \text{K}^{-1}$
T_f (1A)	560.1 ± 0.1	13.09 ± 0.05	23.37 ± 0.09
T_f (1B)	555.7 ± 0.2	12.86 ± 0.03	23.14 ± 0.05
T_g	409.5 ± 0.3		
T_{crys1}	444.3 ± 0.3		
T_{crys2}	525.8 ± 0.4		

^a The kinetic processes, glass transition and crystallizations (T_g , T_{crys1} , and T_{crys2}), were measured at a heating rate of $10 \text{ K} \cdot \text{min}^{-1}$.

technique of solvent-mediated polymorphic transformation.⁶⁶ Thus, if the metastable polymorph is suspended in a saturated solution, the more stable form will then crystallize, due to the lower solubility of the stable polymorph. Several supersaturated solutions of anhydrous LiC_2 (**1A** or **1B**) were prepared, using

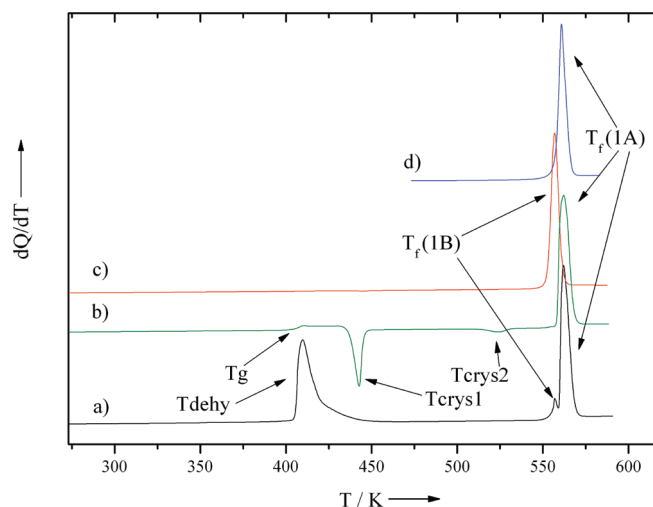


Figure 8. DSC thermograms of (a) compound 2 (quarter-hydrate), showing the dehydration process and the mainly formation of the stable polymorph, **1A**; (b) anhydrous LiC_2 in vitreous state, showing the glass transition (T_g) and both crystallization processes: *crys1* (at T_{crys1}), from the undercooled liquid to the metastable polymorph, **1B**, and *crys2* (at T_{crys2}), from this one to **1A**; (c) anhydrous LiC_2 , corresponding to **1B**, obtained by dehydration of compound 5 (at 428 K for 2 h and cooled down), and showing the melting temperature, $T_f(\text{1B})$; (d) anhydrous LiC_2 , corresponding to **1A**, obtained by cooling the melt at $1 \text{ K} \cdot \text{min}^{-1}$ to 473 K, showing its fusion, $T_f(\text{1A})$.

different solvents or mixtures of them, such as isopropanol, acetonitrile, isopropanol/ethanol (2:1), and isopropanol/methanol (2:1). The formation of different lithium acetate-based solvates in each case was observed by PXRD (Figure 11a–d), so the information found by calorimetry about the stability of the

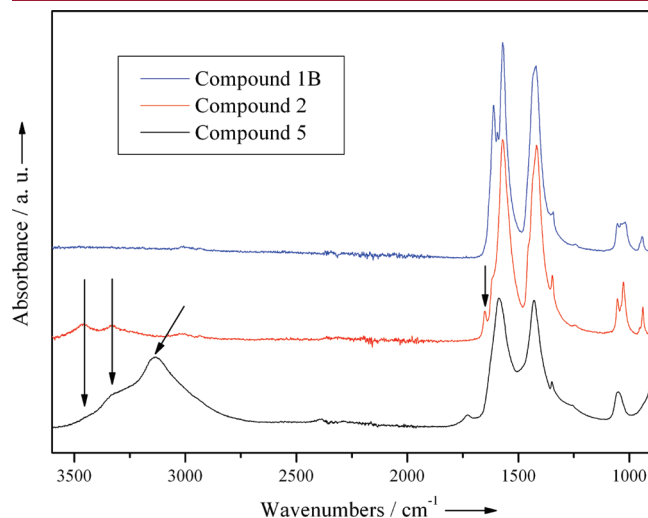


Figure 9. FTIR spectra of compounds 5 (black), 2 (red), and **1B** (blue) at room temperature.

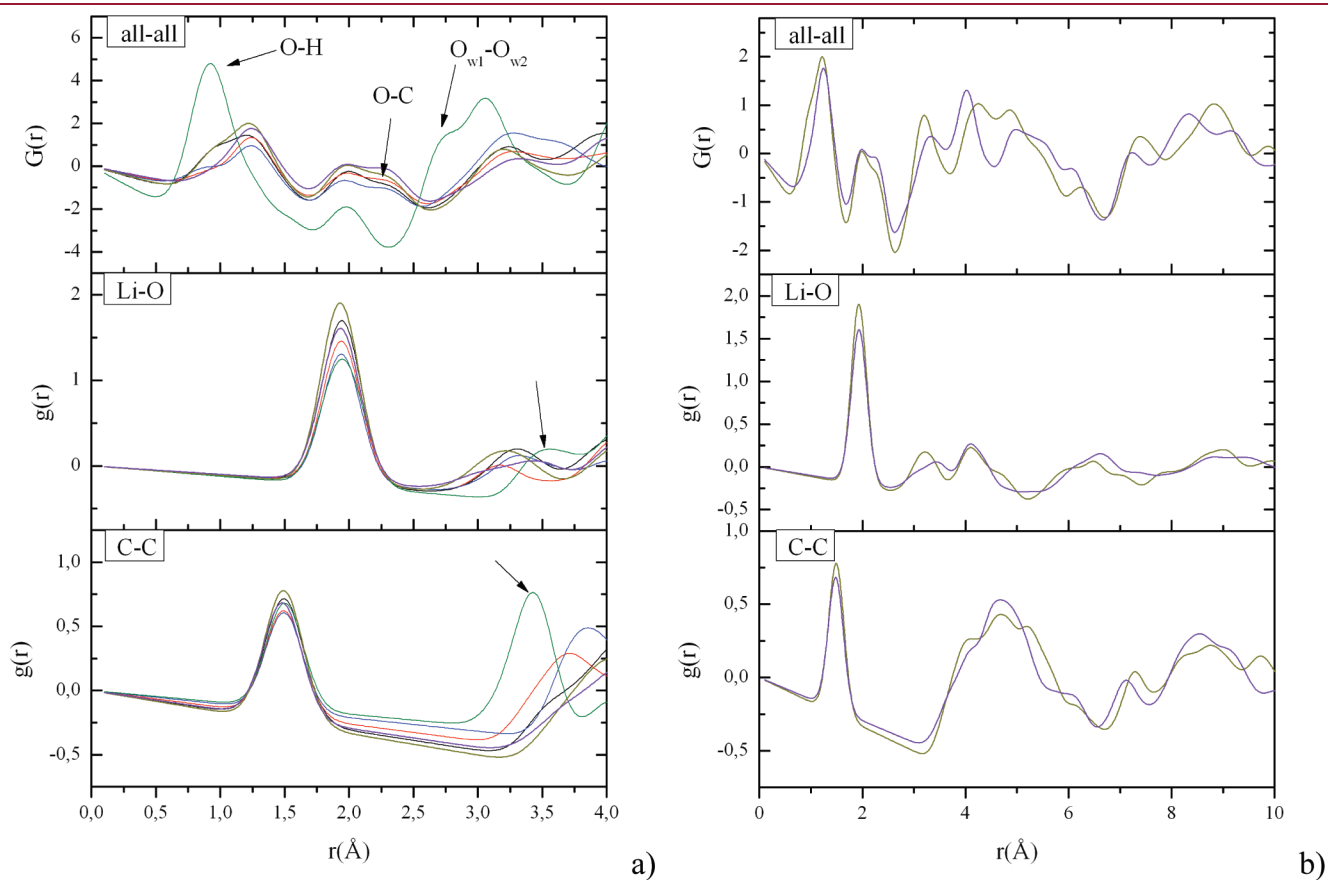


Figure 10. Simulated radial distribution functions, between all atoms, and for the indicated selected atomic pairs, (a) at short distances for compounds **1A**, **1B**, 2, 3, 4, and 5, in thick dark yellow, thick purple, black, red, blue, and green lines, respectively, and (b) at intermediate distances for **1A** and **1B**.

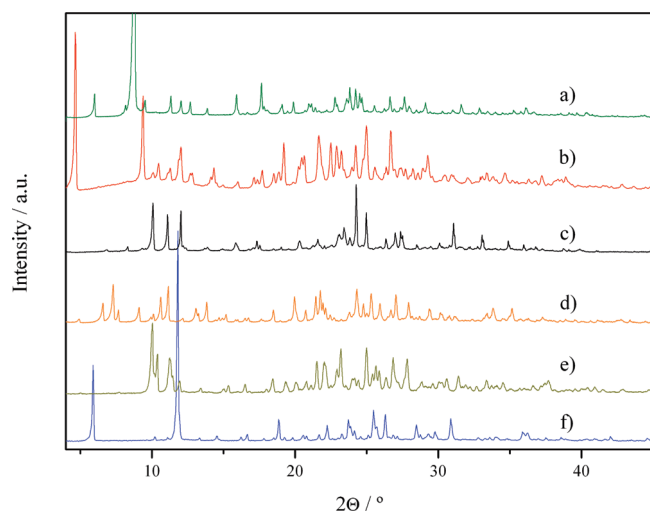


Figure 11. Diffraction patterns of the solvates of LiC_2 obtained from supersaturated solutions of (a) ethanol/isopropanol (1:2), (b) methanol/isopropanol (1:2), (c) isopropanol, and (d) acetonitrile, and from saturated atmospheres of (e) ethanol, and (f) methanol.

polymorphs could not be confirmed by this method. Other two structures were also found by solvation of anhydrous LiC_2 in saturated atmosphere of ethanol and of methanol (Figure 11e,f). These facts show that, besides water, many solvents (or mixtures) might be susceptible to form different LiC_2 -solvates from supersaturated solutions or from anhydrous LiC_2 (**1A** or **1B**) in saturated atmospheres of these solvents.

The selective formation of the two polymorphs of anhydrous LiC_2 by dehydration of different hydrates was also detected by PXRD. Experiments carried out in compounds **2** and **5** showed selective formation of **1A** and **1B** (Figure 12, a and b), respectively, after their dehydration processes. Thus, each hydrate yields one different anhydrous polymorph, compared in Figure 12c, and fitted using the *Fullprof* program⁶⁷ from the crystal structures of **1A** and **1B**. This coincides with the DSC data for compound **2** (Figure 8a) and dehydrated compound **5** (Figure 8c), where the formation of **1A** and **1B**, respectively, was detected.

Finally, comparing both polymorphs, by DSC, XRD, and also in terms of isotropic interatomic distances (radial distribution functions), little differences are detected between them. On the one hand, the enthalpies of both melting processes are almost similar, and the enthalpy of conversion (*crys2*) of **1B** into **1A** is very small. On the other hand, forms **1A** and **1B** share close resemblance in the packing (practically identical densities) and in the arrangement of the LiC_2 molecules ($\text{Li}-\text{O}$ and $\text{Li}-\text{O}-\text{C}$ rings). Consequently, all this information suggests a really small difference in stability between both polymorphs, **1A** and **1B**.

5. CONCLUSIONS

In summary, the new compounds discovered, all of them forming 3D MOFs, reveal a growing interest in lithium acetate. The five new lithium acetate-based structures reported here, anhydrous and hydrated, together with the studies carried out in the last 50 years, demonstrate the complex behavior of an apparently simple salt concerning its relationship with water.

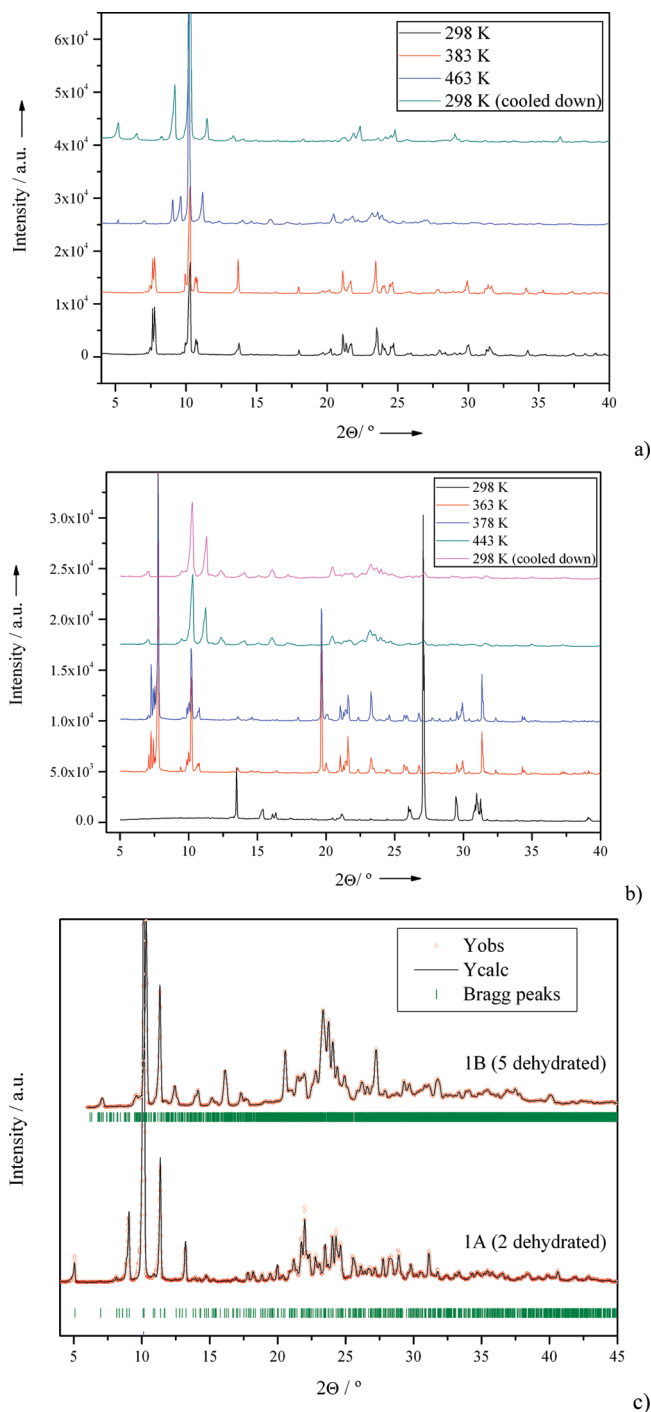


Figure 12. (a) Diffraction patterns of compound **2**, at different temperatures, showing changes after the dehydration process and the final formation of the anhydrous LiC_2 stable polymorph (**1A**); (b) diffraction patterns of compound **5**, at different temperatures, showing changes after the dehydration process and the final formation of the anhydrous LiC_2 metastable polymorph (**1B**); (c) comparison of the diffraction patterns of residues obtained by dehydration of compounds **2–5** (both fitted with the structure of compounds **1A** and **1B**, respectively, solved by SCXRD).

In addition, different solvates of LiC_2 have been detected using other solvents or mixtures.

This study has shown also the existence of monotropic polymorphism, both polymorphs being solved and compared.

They are highly hygroscopic and both present a rather complicated (and unexpected) packing and ionic arrangement for an a priori simple salt, explaining the previous lack of information about the structure of lithium acetate.

This structural study showing the formation of more or less stable new lithium acetate-based compounds (anhydrous, hydrates, and solvates) may help to contribute significantly to a better understanding of this not-so-simple compound, of great importance due to its multiple uses.

■ ASSOCIATED CONTENT

S Supporting Information. Crystallographic information files. This material is available free of charge via the Internet at <http://pubs.acs.org>. The structure reported in this paper may be obtained from the Cambridge Crystallographic Data Center, on quoting the depository numbers CCDC-770300 and CCDC-770301, for **1A** at 100 and 298 K, respectively, CCDC-739978 and CCDC-739979, for **2** at 100 and 298 K, respectively, and CCDC-802905, CCDC-739980, CCDC-739976 and CCDC-739977, for **1B**, **3**, **4** and **5**, respectively (at 100 K).

■ AUTHOR INFORMATION

Corresponding Author

*Laboratorio de Estudios Cristalográficos Edificio Inst. López Neyra Avenida del Conocimiento s/n, P.T. Ciencias de la Salud E-18100 Armilla, Granada, Spain. Tel.: (+34) 958 181621 Lab. 107. Fax: (+34) 958 181632. E-mail: fmarscas@lec.csic.es and BM16, European Synchrotron Radiation Facility (ESRF) 6 rue Jules Horowitz 38043 Grenoble, France. Telephone: (+33) 476882941. Fax: (+33) 476882707. E-mail: fmartine@esrf.fr.

■ ACKNOWLEDGMENT

Partial support of this research by the Beca de Especialización en Organismos Internacionales (ES-2006-0024), by the DGI-CYT of the Spanish Ministerio de Ciencia e Innovación (Project CTQ2008-06328/BQU), by the JAE-DOC postdoctoral grant from the CSIC, are gratefully acknowledged. The authors wish to thank BM16-LLS (Spanish beamline at the ESRF, in Grenoble, France), the CAIs (Centro de Asistencia a la Investigación) of XRD and Spectroscopy of the UCM, the project "La Factoría de Cristalización - CONSOLIDER INGENIO-2010" in Granada (Spain), for the use of their technical facilities. The authors would like to acknowledge A. Labrador and all the BM16 staff, E. Matesanz (UCM), and C. Verdugo (LEC) for their technical assistance during X-ray diffraction experiments.

■ REFERENCES

- (1) Kitagawa, S.; Kitaura, R.; Noro, S. *Angew. Chem., Int. Ed.* **2004**, *43*, 2334–2375.
- (2) Batten, S. R.; Neville, S. M.; Turner, D. R. *Coordination Polymers: Design, Analysis and Application*; Royal Society of Chemistry: London, 2009.
- (3) Mueller, U.; Schubert, M.; Teich, F.; Puetter, H.; Schierle-Arndt, K.; Pastré, J. J. *Mater. Chem.* **2006**, *16*, 626–636.
- (4) Spokoiny, A. M.; Kim, D.; Sumrein, A.; Mirkin, C. A. *Chem. Soc. Rev.* **2009**, *38*, 1218–1227.
- (5) Robin, A. Y.; Fromm, K. M. *Coord. Chem. Rev.* **2006**, *250*, 2127–2157.
- (6) Wong-Foy, A. G.; Matzger, A. J.; Yaghi, O. M. *J. Am. Chem. Soc.* **2006**, *128* (11), 3494–3495.

- (7) (a) Cheon, Y. E.; Suh, M. P. *Angew. Chem.* **2009**, *121*, 2943–2947; (b) *Angew. Chem., Int. Ed.* **2009**, *48*, 2899–2903.
- (8) Ma, S.; Wang, X. S.; Yuan, D.; Zhou, H. C. *Angew. Chem.* **2008**, *120*, 4198–4201.
- (9) Kim, H. J.; Suh, M. P. *Inorg. Chem.* **2005**, *44*, 810–812.
- (10) Lee, J. Y.; Olson, D. H.; Pan, L.; Ernge, T. J.; Li, J. *Adv. Funct. Mater.* **2007**, *17*, 1255–1262.
- (11) Weiner, M. L. Overview of Lithium Toxicology, in *Lithium in Biology and Medicine*; Schrauzer, G. N.; Klippel, K. F., Eds.; VCH Verlag: Weinheim, 1991; pp 83–99.
- (12) Morton, I.; Hall, J. In *Concise Dictionary of Pharmacological Agents: Properties and Synonyms*; Kluwer Academic Publishers: Dordrecht (The Netherlands), 1999.
- (13) Walcher, J.; Schoeckmann, H.; Renders, L. *Kidney Blood Press. Res.* **2004**, *27*, 200–202.
- (14) Brody, J. R.; Kern, S. E. *Anal. Biochem.* **2004**, *333* (1), 1–13.
- (15) Pielichowski, K. *J. Appl. Polym. Sci.* **1999**, *74* (11), 2576–2587.
- (16) (a) Yahya, M. Z. A.; Arof, A. K. *Eur. Polym. J.* **2003**, *39* (5), 897–902. (b) Yahya, M. Z. A.; Arof, A. K. *Carbohydr. Polym.* **2004**, *55* (1), 95–100.
- (17) Arai, H.; Okada, S.; Ohtsuka, H.; Ichimura, M.; Yamaki, J. *Solid State Ion* **1995**, *80*, 261–269.
- (18) Arai, H.; Okada, S.; Sakurai, Y.; Yamaki, J. *Solid State Ion* **1998**, *109*, 295–302.
- (19) Choi, Y. M.; Pyun, S. I.; Moon, S. I.; Hyung, Y. E. *J. Power Sources* **1998**, *72*, 83–90.
- (20) Song, M. Y.; Lee, R. *J. Power Sources* **2002**, *111*, 97–103.
- (21) Santander, N.; Das, S. R.; Majumder, S. B.; Katiyar, R. S. *Surf. Coat. Technol.* **2004**, *177–178*, 60–64.
- (22) Thongtem, T.; Thongtem, S. *Ceram. Int.* **2005**, *31*, 241–247.
- (23) Ningthoujam, R. S.; Umare, S. S.; Sharma, S. J.; Shukla, R.; Kurian, S.; Vatsa, R. K.; Tyagi, A. K.; Tewari, R.; Dey, G. K.; Gajbhiye, N. S. *Hyperfine Interact.* **2008**, *184* (1–3), 227–233.
- (24) Jayakumar, O. D.; Sudakar, C.; Gopalakrishnan, I. K. *J. Cryst. Growth* **2008**, *310*, 3251–3255.
- (25) Finlayson, S. D.; Fleming, C.; Berry, D. R.; Johnson, J. R. *Biotech. Techn.* **1991**, *5* (1), 13–18.
- (26) Antunes, D. F.; de Souza, C. G., Jr.; de Moraes, M. A., Jr. *World J. Microbiol. Biotechnol.* **2000**, *16* (7), 653–654.
- (27) (a) Gietz, R. D.; Woods, R. A. *Methods Mol. Biol.* **2006**, *313*, 107–20. (b) Gietz, R. D.; Schiestl, R. H. *Nat. Protoc.* **2007**, *2* (1), 38–41.
- (28) Penner, G. H.; Hutzal, J. *Magn. Reson. Chem.* **1997**, *35*, 222–226.
- (29) Dhanaraj, P. V.; Rajesh, N. P. *Mater. Chem. Phys.* **2009**, *115* (1), 413–417.
- (30) (a) Nakagawa, T.; Fujisawa, H.; Mukaiyama, T. *Chem. Lett.* **2003**, *32* (5), 462–463. (b) Takahashi, E.; Fujisawa, H.; Mukaiyama, T. *Chem. Lett.* **2004**, *33* (7), 936–937. (c) Nakagawa, T.; Fujisawa, H.; Yuzo, N. I.; Mukaiyama, T. *Chem. Lett.* **2004**, *33* (8), 1016–1017. (d) Nakagawa, T.; Fujisawa, H.; Nagata, Y.; Mukaiyama, T. *Bull. Chem. Soc. Jpn.* **2004**, *77* (8), 1555–1567. (e) Kawano, Y.; Fujisawa, H.; Mukaiyama, T. *Chem. Lett.* **2005**, *34* (4), 614–615. (f) Mukaiyama, T.; Kawano, Y.; Fujisawa, H. *Chem. Lett.* **2005**, *34* (1), 88–89.
- (31) Sauderson, C.; Ferguson, R. B. *Acta Crystallogr.* **1961**, *14*, 321–321.
- (32) Franzosini, P.; Sanesi, M.; Cingolani, A.; Ferloni, P. Z. *Naturforsch.* **1980**, *35a*, 98–102(b); c).
- (33) Franzosini, P.; Sanesi, M. *Thermodynamic and Transport Properties of Organic Salts*; Pergamon Press: Oxford, 1980.
- (34) Ferloni, P.; Westrum, E. F. *Pure Appl. Chem.* **1992**, *64* (1), 73–78.
- (35) Cheda, J. A. R.; Redondo, M. I.; García, M. V.; López de la Fuente, F. L.; Fernández-Martín, F.; Westrum, E. F. *J. Chem. Phys.* **1999**, *111*, 3590–3598.
- (36) Martínez Casado, F. J.; García Pérez, M. V.; Redondo Yélamos, M. I.; Cheda, J. A. R.; Sánchez Arenas, A.; López de Andrés, S.; García-Barriocanal, J.; Rivera, A.; León, C.; Santamaría, J. J. *Phys. Chem. C* **2007**, *111* (18), 6826–6831.

- (37) Martínez Casado, F. J.; Ramos Riesco, M.; Sánchez Arenas, A.; García Pérez, M. V.; Redondo, M. I.; López-Andrés, S.; Garrido, L.; Cheda, J. A. R. *J. Phys. Chem. B* **2008**, *112* (51), 16601–16609.
- (38) Amirthalingam, V.; Padmanabhan, V. M. *Acta Crystallogr.* **1958**, *11*, 896–896.
- (39) Clark, J. R. *Acta Crystallogr.* **1964**, *17*, 459.
- (40) Galigné, J. L.; Mouvet, M.; Falgueirettes, J. *Acta Crystallogr. B* **1970**, *26*, 368–372.
- (41) Kearley, G. J.; Nicolai, B.; Radaelli, P. G.; Fillaux, F. J. *Solid State Chem.* **1996**, *126*, 184–188.
- (42) Meisingset, K. K.; Grønvdal, F. J. *Chem. Thermodyn.* **1984**, *16*, 523–536.
- (43) Tobón-Zapata, E.; Ferrer, E. G.; Etcheverry, S. B.; Baran, E. J. *J. Therm. Anal. Calorim.* **2000**, *61*, 29–35.
- (44) Crits, E.; Van Gerven, L.; Emid, S. *Physica B* **1988**, *150*, 329–336.
- (45) Stevens, K. W. H. *J. Phys. C: Solid State Phys.* **1983**, *16*, 5765–5772.
- (46) Nicolai, B.; Cousson, A.; Fillaux, F. *Chem. Phys.* **2003**, *290*, 101–120.
- (47) Schiebel, P.; Kearley, G. J.; Johnson, M. R. *J. Chem. Phys.* **1998**, *108*, 2375–2382.
- (48) Iwasaki, M.; Toriyama, K. *J. Chem. Phys.* **1985**, *82*, 5415–5423.
- (49) Kansikas, J.; Hermansson, K. *Acta Crystallogr. C* **1989**, *45*, 187–191.
- (50) Muller, K.; Heyns, A. M.; Range, K. J.; Zabel, M. Z. *Naturforsch., B: Chem. Sci.* **1992**, *47*, 238–246.
- (51) Rao, J. K. M.; Viswamitra, M. A. *Ferroelectrics* **1971**, *2* (3), 209–216.
- (52) Enders-Beumer, A.; Harkema, S. *Acta Crystallogr. B* **1973**, *29*, 682–685.
- (53) Martínez Casado, F. J.; Ramos Riesco, M.; García Pérez, M. V.; Redondo Yélamos, M. I.; López-Andrés, S.; Cheda, J. A. R. *J. Phys. Chem. B* **2009**, *113* (39), 12896–12902.
- (54) Martínez Casado, F. J.; Ramos Riesco, M.; Da Silva, I.; Redondo, M. I.; Labrador, A.; Cheda, J. A. R. *Cryst. Growth Des.* DOI: 10.1021/cg101272n.
- (55) Martínez Casado, F. J.; Ramos Riesco, M.; Da Silva, I.; Labrador, A.; Redondo, M. I.; García Pérez, M. V.; López-Andrés, S.; Cheda, J. A. R. *J. Phys. Chem. B* **2010**, *114* (31), 10075–10085.
- (56) Ehrenberg, H.; Hasse, B.; Schwarzb, K.; Eppe, M. *Acta Crystallogr. B* **1999**, *55*, 517–524.
- (57) Sheldrick, G. M. *Acta Crystallogr.* **2008**, *A64*, 112–122.
- (58) Lutz, H. D. In *Bonding and Structure of Water Molecules in Solid Hydrates. Correlation of Spectroscopic and Structural Data*; Springer: Berlin/Heidelberg, 1988; pp 97–125.
- (59) Onodera, N.; Suga, H.; Seki, S. *Bull. Chem. Soc. Jpn.* **1968**, *41* (9), 2222.
- (60) Farrow, C. L.; Juhás, P.; Liu, J. W.; Bryndin, D.; Božin, E. S.; Bloch, J.; Proffen, Th.; Billinge, S. J. L. *J. Phys.: Condens. Matter* **2007**, *19*, 335219.
- (61) Ramos Riesco, M.; Martínez Casado, F. J.; López-Andrés, S.; García Pérez, M. V.; Redondo Yélamos, M. I.; Torres, M. R.; Garrido, L.; Rodríguez Cheda, J. A. *Cryst. Growth Des.* **2008**, *8* (7), 2547–2554.
- (62) Sato, K.; Kobayashi, W. In *Crystals, Growth, Properties and Applications: Organic Crystals*; Kare, Ed.; Springer-Verlag: Berlin, 1991; Vol. 1, pp 65–108.
- (63) Gu, C.-H.; Young, V., Jr.; Grant, D. J. W. *J. Pharm. Sci.* **2001**, *90* (11), 1878–1890.
- (64) Takata, N.; Shiraki, K.; Takano, R.; Hayashi, Y.; Terada, K. *Cryst. Growth Des.* **2008**, *8* (8), 3032–3037.
- (65) Ostwald, W. *Z Phys. Chem.* **1897**, *22*, 289–330.
- (66) Rodríguez-Hornedo, N.; Murphy, D. J. *J. Pharm. Sci.* **1999**, *88* (7), 651–660.
- (67) (a) Rodríguez-Carvajal, J. *Physica B* **1993**, *192*, 55–69. (b) Rodríguez-Carvajal, J. *Commission on Powder Diffraction (IUCr) Newsletter* **2001**, *26*, 12–19.